Energy pumping-and-damping for gait robustification of underactuated planar biped robots within the hybrid zero dynamics framework

Pierluigi Arpenti[1], Alejandro Donaire[2], Fabio Ruggiero[1], and Vincenzo Lippiello[1]

***Abstract*— This paper addresses the robust gait control for planar and passive biped robots using approaches based on energy properties. Energy pumping-and-damping passivity-based control is used to increase the robustness against uncertainties on the initial conditions of the passive gait exhibited by planar biped robots. The stability analysis is carried out by exploiting the system's passivity and the hybrid zero dynamics method. Besides, the proposed approach is applied to new gaits that are generated using interconnection and damping assignment passivity-based control. The performance of the proposed design is evaluated through numerical simulations and compared with an existing technique.**

I. Introduction

Firstly studied in [1], passive dynamic walking is the stable walk exhibited by a planar biped robot descending a shallow slope under the gravitational field's effect only. Planar biped robots are commonly studied as hybrid systems, characterized by continuous dynamics (usually referred to as swing phase) alternating with discrete events (the foot strikes). During the swing phase, if non-conservative forces are absent, the system's total energy is conserved, and dissipation only occurs when a foot lands on the ground and non-conservative forces arise. Passive dynamic walking originates from the mechanical energy conservation during the swing phases, and from the restoration of the potential energy to its initial value at the end of every single step. This comes out from the inelastic impacts with the ground dissipating the kinetic energy gained during the swing phase. Ideally, if both the robot and the environment meet particular geometrical and inertial conditions, the whole process can evolve indefinitely [1], [2], [3], [4].

The study of passive dynamic walking attracted many researchers due to the similarities with human gait features, serving as a testbed to investigate human locomotion [5], [6]. Moreover, from an energetic viewpoint, exploiting the passivity of such kind of motion means designing more efficient control strategies compared to the other state-of-the-art biped locomotion control approaches based on walking primitives pre-planning and the zero moment point stability criterion [7].

Energy shaping is a method belonging to the class of passivity-based control (PBC) techniques that exploit the intrinsic physical and passive properties of the systems [8]. It was proved to be an effective, though poorly used, strategy to control passive walkers. Passive (uncontrolled) gaits suffer from weak stability properties since the associated limit cycles (*i.e.*, the solutions representing the gaits in the phase plane) usually exhibit a restricted basin of attraction. Therefore, the advantage of shaping the energy during continuous dynamics is twofold. First, the passive gait's basin of attraction can be enlarged. Second, the gait can be modified by changing the way the robot and the ground exchange energy [9], [10], [11], [12]. All the works cited so far exploit methodologies (*e.g.*, the controlled symmetries (CS) and the controlled Lagrangians (CL)), which are based on the Lagrangian modeling framework. Recently, the port-Hamiltonian (pH) modeling framework was shown to be efficient in designing PBC strategies by explicitly taking into account the system's energy. The first attempt to exploit the pH framework was proposed in [13]. Later, a control strategy based on the interconnection and damping assignment passivity-based control (IDA-PBC) [14], [15], capable of generating robust gaits characterized by small step lengths and slow forward speed, was proposed in [7]. An underactuated compass-like biped robot (CBR) was instead controlled through the IDA-PBC in [16], without solving the partial differential equations that usually characterize such a control methodology and without requiring any change of coordinates as in [7].

The revised methodologies ignore the hybrid nature of the system during control synthesis. Passivity-based control frameworks have been developed to control mechanical systems in absence of impacts. Ensuring asymptotic stability to the desired energy level generally suffices to such a class of systems. IDA-PBC guarantees that target dynamics are asymptotically stabilized at an equilibrium point corresponding to the minimum of the target Hamiltonian, for instance. As outlined in [17] and [18], the methods stabilizing a biped robot to a specific gait construct a zero dynamics manifold. The reset map characterizing hybrid systems pushes away solutions that do not lie in the zero dynamics manifold [17], [19]. Hence, the convergence of the continuous dynamics to the manifold must be sufficiently rapid to counteract the repulsive behavior of the reset map. CS, CL, and IDA-PBC neither construct a zero dynamics manifold nor guarantee exponential convergence of continu-

The research leading to these results has been supported by both the PRINBOT project (in the frame of the PRIN 2017 research program, grant number 20172HHNK5_002) and the WELDON project (in the frame of Programme STAR, financially supported by UniNA and Compagnia di San Paolo). The authors are solely responsible for its content.

[1]Pierluigi Arpenti, Fabio Ruggiero, and Vincenzo Lippiello are with the PRISMA Lab, Department of Electrical Engineering and Information Technology, University of Naples, Via Claudio 21, 80125, Naples, Italy. Contact emails {pierluigi.arpenti, fabio.ruggiero, vincenzo.lippiello}@unina.it

[2]Alejandro Donaire is with the School of Engineering, Faculty of Engineering and Built Environment, The University of Newcastle, University Drive, Callaghan, 2308, NSW, Australia alejandro.donaire@newcastle.edu.au

ous dynamics to it. Hence, they can stabilize the biped robot to neither a specific gait nor a target energy level (due to the presence of impacts), while they effectively generate new gaits. The approaches that duly take into account the hybrid nature of the system should address closed-loop exponential stability [17]. Some of them ensure exponential convergence by exploiting the notion of hybrid zero dynamics (HZD) [20], [21], [22]. While these preliminary works were based on an input-output linearization, an approach based on a Lyapunov analysis was proposed in [19], where rapidly exponentially stabilizing control Lyapunov functions (RES-CLF) were used to make the output dynamics converge exponentially fast to the HZD manifold with a rate of convergence which can be modified by gain adjustments. Later, the same framework was extended in [18] to achieve energy-shaping to increase the robustness of the passive gait of the CBR to perturbations in initial conditions. Based on the HZD, but not relying on RES-CLF, the work in [23] proposed a passivity-based approach to keep the natural dynamics of the system and enhance the performance in terms of robustness and control effort minimization.

This paper uses HZD and energy pumping-and-damping passivity-based control (EPD-PBC) [24] to achieve exponential stabilization to a reference energy value for a planar passive walker. A variant of the EPD-PBC was proposed in [25] as a modification of the IDA-PBC to generate stable limit cycles for pH systems meeting specific requirements on the model structure. Besides, the EPD-PBC was exploited in [26] to generate new gaits for a CBR through dissipative forces. Differently from the approach presented in this work, the hybrid nature of the system was not explicitly taken into account during controller design in [26]. The target energy in the EPD-PBC can be related to the passive gait or another one if an inner energy shaping control loop is applied. The use of energy shaping is motivated since it is necessary to change the way the robot and the ground exchange energy [4]. Because of the pH formalism and the biped underactuation, IDA-PBC will be here exploited.

The paper's contributions are now listed. *i)* The control strategy used to exponentially stabilize the system to a target energy value is well known in the literature since it has been already used to tackle several control tasks. Nevertheless, to the best of the authors' knowledge, this is the first time that it has been used within the HZD framework. This represents the first attempt to join energy-based methodologies, rooted in the pH formalism, with an approach explicitly developed to control biped robots. *ii)* The proposed control strategy can be used without any further modification combined with an energy-shaping control strategy to modify the system's total energy, enlarging the spectrum of potentially achievable robust gaits. *iii*) The stability analysis is based on the invariant set theory rather than Poincaré maps, leading to less conservative [27] and almost global results.

II. Problem Description

Conservation of energy is the physical principle that motivates passive dynamic walking [1], [3]. Consequently, a limit cycle can be regarded as an energy-conserving orbit corresponding to a specific mechanical energy value $E^* \in \mathbb{R}$ [1], [2], [3], [4], [18]. One of the main drawbacks of limit cycle walking is finding the correct set of initial conditions, such as triggering the limit cycle. Besides, initial conditions related to a limit cycle are extremely sensitive to perturbations. The objective of this work is to provide a methodology to extend the range of possible initial conditions leading to periodic walking, *i.e.*, to enlarge the basin of attraction of a given limit cycle. As shown in [18], one possible approach is to build an output variable, namely $e = E(x) - E^*$, with $E(x) \in \mathbb{R}$ the energy of the system. Suppose that the system has been written in the hybrid zero dynamics form, as in [18]. If the output dynamics $\dot{e}$ converge exponentially fast to zero, then, based on results about HZD for planar bipeds [20], [21], the set of states such that $e = 0$ and $\dot{e} = 0$ constitutes a hybrid invariant zero dynamics manifold. Such states are those for which $E(x) = E^*$, hence the system has been exponentially stabilized at the energy level E^* with the beneficial effects that its basin of attraction has been enlarged, as illustrated in [18]. To prove stability for the overall system, Poincaré maps are used in [18]. One drawback of employing such a method is that it recasts the stability analysis to a standard equilibrium stabilization problem, leading to very conservative results [27]. Conversely, it is better to exploit the notion of stability of an invariant set, which is the closed orbit associated with the periodic solution [25], [27]. Moreover, since the Poincaré maps require linearizing the system at the fixed point, they hold only locally in a neighborhood of the point. This is in contrast with the target of this paper, that aims at enlarging the periodic solution's basin of attraction. Indeed, invariant-set theorems lead to global or almost global stability results [28]. In the next sections, it will be shown how an existing control methodology, namely the EPD-PBC, can be designed to overcome the limitations of the approach presented in [18], in the sense that it yields less conservative stability results based on the invariant-set theory.

III. Technical Background

A. Hybrid Systems and Underactuated Mechanical Systems in pH Formalism

In this paper, the following hybrid system with impulse effects

$$\begin{cases} \dot{x} = f_1(x) + g_1(x)u(x) & x \in X \backslash S \\ x^+ = \Delta(x^-) & x^- \in S \end{cases} \tag{1}$$

is considered, where $x \in X$ is the state, x^- and x^+ indicate the states just before and after an impact, respectively, $X \subseteq \mathbb{R}^N$ is the admissibility domain of continuous dynamics with cardinality N, $f_1 : X \to X$ is the C^1 vector field describing continuous dynamics, $g_1 : X \to X$ is the C^1 vector field mapping the control input $u(x)$ to the continuous dynamics, S is the switching surface, and $\Delta : S \to X$ is the C^1 reset map.

Consider an underactuated mechanical system with n degrees of freedom and $m = n - 1$ control inputs. Let $q \in \mathbb{R}^n$ and $p \in \mathbb{R}^n$ be the vector of generalized coordinates and

momenta, respectively. Let $H(q,p):\mathbb{R}^{2n}\to\mathbb{R}$ be the Hamiltonian function, $H(q,p)=\frac{1}{2}p^TM^{-1}(q)p+V(q)$, expressing the total mechanical energy stored in the system given by the sum between kinetic and potential energy, $V(q)\in\mathbb{R}$. The pH model of such underactuated mechanical system is

$$\begin{bmatrix}\dot{q}^T & \dot{p}^T\end{bmatrix}=J(q,p)\nabla H(q,p)+G(q)u(q,p), \tag{2}$$

where $J(q,p)=-J^T(q,p)\in\mathbb{R}^{2n\times 2n}$ is the skew-symmetric interconnection matrix mapping the principle of conservation of energy. The control input $u(q,p)\in\mathbb{R}^m$ is modulated by the input mapping matrix $G(q)=\begin{bmatrix}0_{m\times n} & G_p^T(q)\end{bmatrix}^T$, where $G_p\in\mathbb{R}^{n\times m}$ is a full rank matrix.

Biped robots with rotating point feet belong to the class of underactuated mechanical systems [17, Section 3.4]. Point-feet synthesizes some of the properties encompassed by human feet although they are more difficult to be controlled. This work deals with planar biped robots equipped with unactuated point-feet because they represent an interesting case study for any locomotion control design methodology [17]. During the swing phase, the stance leg is continuously in contact with the ground, behaving like a pivot. The other one, the swing leg, moves freely in the air. Therefore, the interaction between the stance foot and the ground is uncontrolled, yielding to one degree of underactuation in the related model. Swing dynamics are modeled through the pH formalism, as in (2). This choice is motivated by the relationship connecting energy and dynamics, which has given room to plenty of energy shaping control methodologies well suited for underactuated mechanical systems.

Remark. *$J(q,p)$ in* (2) *has been expressed in a general form intentionally, without assuming any particular structure for it. With such a choice, it can represent both uncontrolled and controlled mechanical systems, as long as the latter ones preserve the principle of conservation of energy characterizing uncontrolled systems. This can be achieved using an energy shaping control action, carried out by IDA-PBC, for instance, like the one that will be employed in the Case Study II of Section V.*

B. Energy Pumping-And-Damping PBC

A general way to define an EPD-PBC controller for a pH system is through the following control action [24], [26]

$$u_{pd}(q,p)=-K_{pd}e(q,p)G_p^T(q)\nabla_p H(q,p), \tag{3}$$

where $K_{pd}\in\mathbb{R}^{m\times m}$ is a positive definite gain matrix and $e\in R$ is a suitable scalar variable depending on q and p. This must be appropriately selected such that

$$e(q,p)=\begin{cases}e(q,p)=0 & \text{if } (q,p)\in Z,\\ e(q,p)\neq 0 & \text{if } (q,p)\in\mathbb{R}^{2n}-Z,\end{cases} \tag{4}$$

where $Z\subset\mathbb{R}^{2n}$ is a given subset of the state-space which has to be defined. Substituting (3) in (2) yields the closed-loop system

$$\begin{bmatrix}\dot{q}^T & \dot{p}^T\end{bmatrix}=[J(q,p)+R_{pd}(q,p)]\nabla H(q,p) \tag{5}$$

where

$$R_{pd}(q,p)=\begin{bmatrix}O_n & O_n\\ O_n & -G_p(q)K_{pd}e(q,p)G_p^T(q)\end{bmatrix}\in\mathbb{R}^{2n\times 2n} \tag{6}$$

is the pumping-and-damping matrix. $R_{pd}(q,p)$ is positive definite in some regions of the state space, it is negative definite in other ones, and it is zero only when $e(q,p)=0$.

IV. Controller Design

A. EPD-PBC Design within HZD Formulation

Let $N=2n$ and $x=(q,p)\in\mathbb{R}^{2n}$. The continuous dynamics (1) is modeled as the continuous pH system (2), that is

$$f_1(x)+g_1(x)u=J(x)\nabla H(x)+G(x)u(x). \tag{7}$$

Designing $u(x)=u_{pd}(x)$ in (3), with

$$e=H(x)-H^*, \tag{8}$$

where $H^*\in\mathbb{R}$ is a constant target Hamiltonian, the hybrid system (1) with the continuous dynamics (7), the control input (3), and the output variable (8) is

$$\begin{cases}\dot{x}=f_1(x)+g_1(x)u_{pd}(x,e) & (x,e)\in X\backslash S,\\ \dot{e}=f_2(x)+g_2(x)u_{pd}(x,e) & (x,e)\in X\backslash S,\\ x^+=\Delta(x^-) & (x^-,e^-)\in S,\\ e^+=\Delta(e^-) & (x^-,e^-)\in S,\end{cases} \tag{9}$$

where $f_1(x)=J(x)\nabla H(x)$, $f_2(x)=\nabla_x H(x)^TJ(x)\nabla_x H(x)$, $g_1(x)=G(x)$, and $g_2(x)=\nabla_x H(x)^TG(x)$ are assumed to be locally continuous Lipschitz functions. Notice that the first equation in (9) can be equivalently written as in (5). Variable e is usually referred to as *output* (sometimes also called *transverse variable*), while x are referred to as zero dynamics variables [19]. The dependence of u_{pd} on e has been been made explicit in (9). The zero dynamics submanifold is the restricted subset $Z\subset X$ defined as $Z=\{x\in X|e=0\}$. Additionally, if $\dot{e}=0$, then the zero dynamics submanifold Z is forward invariant (*i.e.*, it is invariant under the swing dynamics only). If the biped is planar, it is sufficient to guarantee the exponential convergence of the output dynamics to Z and make it hybrid invariant, that is invariant under both swing dynamics and foot-strikes [21], [22].

As consequence of (8), the sign of the pumping-and-damping matrix $R_{pd}(x)$ changes accordingly to the actual value of $H(x)$ respect to the target value H^*. The following condition

$$R_{pd}(x)e=-G_p(q)K_{pd}G_p^T(q)e^2\leq 0 \tag{10}$$

always holds true.

B. Zero Dynamics Stability Analysis

The goal of this section is to show that, through (3), the zero dynamics submanifold is both forward invariant and attractive, and that the closed-loop system (9) is exponentially stable to it.

Firstly, assume that Z is the largest invariant in the set

$$\{x\in X|\nabla_x^TH(x)R_{pd}(x)\nabla_x H(x)e=0\}. \tag{11}$$

To prove the exponential stability of the closed-loop system (9) respect to Z, the storage function

$$V(e) = \frac{1}{2}e^2 \geq 0, \tag{12}$$

positive everywhere except for $e = 0$, is selected. The output variable e constitutes an isolated minimum for the storage function $V(e)$ in the zero dynamics submanifold Z, that is

$$\begin{aligned} &\nabla_e V(e)|_{x\in Z} = e|_{x\in Z} = 0, \\ &\nabla_e^2 V(e)|_{x\in Z} = 1 > 0. \end{aligned} \tag{13}$$

Then, the time derivative of $V(e)$ is

$$\dot{V}(e) = \frac{\partial V(e)}{\partial e}\dot{e} = e\dot{e}, \tag{14}$$

while the time derivative of the output dynamics is

$$\begin{aligned} \dot{e} &= \dot{H}(x) - \dot{H}^* = \nabla_x H(x)^T \dot{x} \\ &= \nabla_x H(x)^T (J(x) + R_{pd}(x))\nabla_x H(x) \\ &= \nabla_x H(x)^T R_{pd}(x)\nabla_x H(x) \\ &= -\nabla_p H(x)^T G_p(q) K_{pd}\ e\ G_p^T(q)\nabla_p H(x) \\ &= -l(x)e, \end{aligned} \tag{15}$$

with $l(x) = \nabla_p H(x)^T G_p(q) K_{pd} G_p^T(q)\nabla_p H(x) \geq 0$. Notice that $J(x)$ has been exploited to cancel out the related quadratic term. Substituting (15) into (14) yields

$$\begin{aligned} \dot{V}(e) &= -\nabla_p H(x)^T G_p(q) K_{pd} e^2 G_p^T(q)\nabla_p H(x) \\ &= -2l(x)\frac{1}{2}e^2 = -2l(x)V(e) \leq 0. \end{aligned} \tag{16}$$

Relation (16) with (13) proves the exponential stability of (9) with respect to Z. Given (13), the following holds

$$\nabla^T H_x(x) R_{pd}(x)\nabla H_x(x) e|_{x\in Z} = 0. \tag{17}$$

Attractivity of Z is proved applying LaSalle's invariance principle, taking into account (16) and the assumption (11).

To prove the forward invariance of Z, the restriction of the transverse dynamics to the zero dynamics submanifold must be considered

$$\dot{e}|_{x\in Z} = f_2(x)|_{x\in Z} + g_2(x)u_{pd}(x,e)|_{x\in Z}. \tag{18}$$

Since $e = 0$ in Z, then $u_{pd}(x,0)|_{x\in Z} = 0$. Besides, since $\dot{e} = \dot{H}(x)$, (18) can be rewritten as $\dot{H}(x)|_{x\in Z} = f_2(x)|_{x\in Z}$. Since the mechanical energy is constant during swing dynamics due to the absence of dissipation, then $\dot{e}|_{x\in Z} = \dot{H}(x)|_{x\in Z} = 0$ holds, proving the forward invariance of Z which, now, can be profitably defined as

$$Z = \{x \in X | e = 0, \dot{e} = 0\}. \tag{19}$$

Finally, hybrid invariance is automatically achieved in (15), where output dynamics convergence exponentially fast to Z, under the control law (3). Moreover, the exponential rate of convergence can be adjusted by profitably tuning the gain matrix K_{pd} in $l(x)$.

The benefits of such results are twofold.

1) Suppose that a limit cycle exists and it is a periodic solution of the zero dynamics. In that case, if the related mechanical energy belongs to the zero dynamics submanifold, its stability is automatically guaranteed by using the stability theory of invariant sets, instead of Poincaré map analysis [25].
2) The stability of the closed-loop system restricted to the zero dynamics is the prerequisite to guarantee the stability of the closed-loop system's full-order dynamics.

C. Full-Order System Stability Analysis

The results of the previous section hold only for the hybrid zero dynamics and the associated submanifold Z. Once that the exponential stability of a periodic solution is guaranteed, and that such a property is valid under continuous and discrete dynamics, this result must be transferred to the full order system, *i.e.*, system (9) not restricted to Z. Since (9) meets the hypotheses outlined in [23], it is possible to conclude that the exponential stability of a periodic orbit belonging to the hybrid restriction dynamics implies the exponential stability of the same periodic orbit for the full-order system (for the detailed demonstration, see [23]). In particular, the following conditions must be verified.

1) For Z in (19), $S \cap Z$ is a $(2n-1)$ dimensional hybrid invariant submanifold of Z.
2) System (9) has a exponentially stable periodic orbit O contained in Z, which is transverse to the reset map S.
3) The storage function $V(e)$ is positive definite locally around the orbit O, it decreases during swing dynamics as showed in (16), and its value is zero on the orbit.
4) If the scalar e is measured right after any impact and it is defined as e_i, where i stands for the $i-th$ impact event, then the sequence of the storage functions $V(e_i)$, evaluated at every impact, is decreasing.

The first condition is true because Z is a hybrid invariant submanifold. Conditions 2 and 3 above are satisfied if the energy value of a given periodic orbit O, transverse to S by hypothesis, belongs to Z, as demonstrated in (16). Finally, since an uncontrolled passive walker dissipates kinetic energy at every impact (supposed perfectly inelastic), while mechanical energy is constant during swing dynamics, $H(x)$ decreases to the passive value at every foot strike. When the biped is controlled using $u_{pd}(x)$ in (3), with e in (8), the only effect is in the swing phase, where $V(e)$ exponentially decreases to zero as pointed out in (16). Hence, summing up the dissipation during the continuous dynamics, achieved via control, and the dissipation naturally taking place at discrete events, the consequence is that $V(e_i)$ constitutes a decreasing sequence of values.

V. Case Studies

In this section, numerical simulations are carried out to evaluate the performance of the proposed approach.

The CBR depicted in Fig. 1 is used with parameters $m_H =$ 10 kg, $m = 5$ kg, $a = 0.5$ m, $b = 0.5$ m, $g = 9.8$ m/s^2, and $\phi =$ 3 deg. More details about the CBR can be found in [12], [16]. The CBR state is described by $q_1 \in \mathbb{R}$, which is the stance leg variable, and by $q_2 \in \mathbb{R}$ which is the hip variable reported to the swing leg. Both of them are calculated with respect to

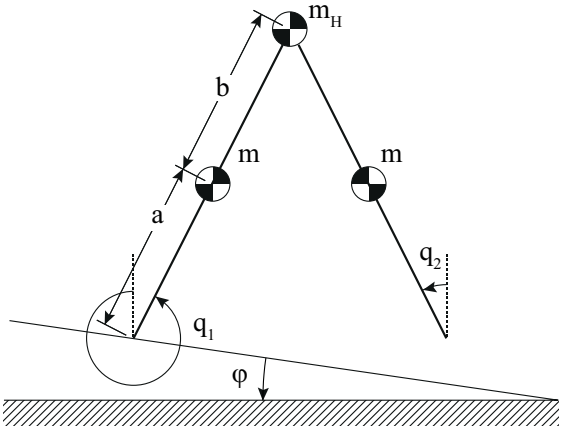

Fig. 1. Physical idealization of the CBR.

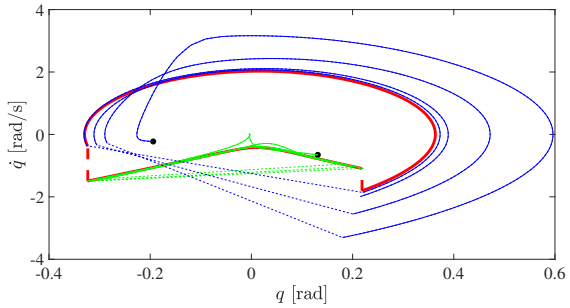

Fig. 2. Case Study I. Limit cycle comparison. Red arcs represent the passive limit cycle. Green arc represents the component of the limit cycles relative to q_1, while blue arc represents the component of the limit cycles relative to q_2 during a test carried out starting by perturbed initial conditions. Black dots represent initial conditions. Both green and blue arcs converge to red ones using EPD-PBC with $k_{pd} = 8.4$.

the vertical to the ground. The robot is underactuated with the control torque applied only at the hip joint.

The simulations are performed on a standard personal computer in the MATLAB environment. The dynamic model of the CBR is numerically simulated through the *ODE*45 routine of MATLAB with the event detection option active to evaluate the foot-ground hit. The designed controller is implemented at a discrete-time step of 0.01 s. The average computation time of the controller is ≈ 0.12 ms with a standard deviation of ≈ 0.41 ms. The simulations last 20 s. In the literature, a step is defined as two consecutive foot-ground impacts [3], [7], [12]. Then, two parameters characterize the gaits of the CBR: the space covered on the slope by each step, which is referred to as *step length*, $S > 0$, and its duration, which is referred to as *step period*, $T > 0$.

A. Case Study I

In the first case study, only the EPD-PBC is applied, without any energy shaping, to test the performance in terms of robustification of the passive gait to perturbed initial conditions. Passive gait is exhibited by the CBR without control, starting by the initial conditions $x_{0P} = \begin{bmatrix} 0.2187 & -0.3234 & -1.0918 & -0.3772 \end{bmatrix}^T$ where the first two components are the generalized coordinates, while the last two are the generalized velocities. Initial conditions have been defined in terms of coordinates and velocities (as in [18]) rather than in terms of coordinates and momenta. Notice that the momenta are linearly related to the velocities through the inertia matrix. Passive gait parameters are known to be $S_P = 0.5347$ m, $T_P = 0.7347$ s, $H_P = 153.0787$ J for the chosen CBR [4].

EPD-PBC enlarges the basin of attraction of the passive gait. Firstly, uniform perturbations on initial conditions have been considered. Three distinct sets of perturbed initial conditions were obtained multiplying x_{0P} by 0.8 (small perturbation), 0.7 (medium perturbation), and 0.6 (large perturbation), respectively [18]. The control gain for each initial condition has been experimentally tuned as $k_{pd} = 1$, $k_{pd} = 10.2$, and $k_{pd} = 8.4$, respectively.

Fig. 2 shows the limit cycle in the phase plane of the controlled CBR starting from $0.6x_{oP} = \begin{bmatrix} 0.1312 & -0.1940 & -0.6551 & -0.2263 \end{bmatrix}^T$ with $k_{pd} = 8.4$. Both the part of the cycle related to the swing angle (blue line) and the one associated with the stance angle (green line) converge to the passive limit cycle (red line). The CBR recovers the passive gait after a large perturbation on the initial state thanks to EPD-PBC, which thus enlarges the basin of attraction of the passive limit cycle. The periodic motion associated with the first leg, which is the swing one at the beginning of the simulation, is depicted in Fig. 3 (since the gait is symmetric, this figure holds for the other leg also, though with a different initial condition).

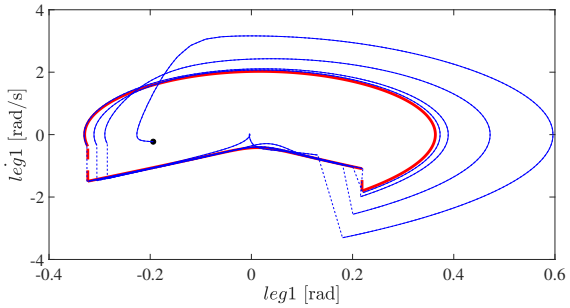

Fig. 3. Case Study I. Limit cycles comparison for the first leg. Red arcs represent the passive limit cycle. Same legend and condition of Fig. 2 hold.

Fig. 4 shows the convergence of the storage function $V(e)$ to zero. At every impact, the value of $V(e)$ is smaller than (or equal to) the value of the same function at the previous foot strike. This gives a numerical confirmation that the passivity of the switched systems is a right hypothesis.

To further enlighten an increment of robustness to initial conditions, nonuniform perturbations have been taken into account (*i.e.*, distinct perturbations on every component of x_{0P} were considered). Ten further simulations have been carried out, each one starting from a different initial condition x_{0P_i} with $i = 1, \ldots, 10$, obtained multiplying x_{0P} by as many diagonal matrices whose elements have been randomly computed to lie in the set $\{0.8, 0.7, 0.6\}$. For the

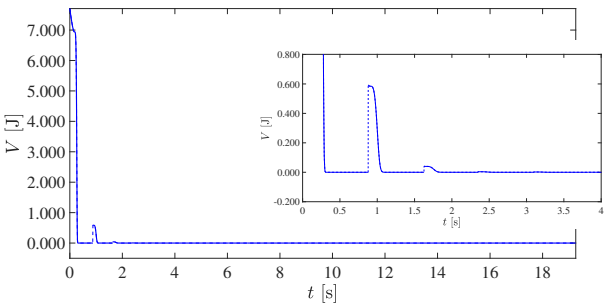

Fig. 4. Case Study I. Storage function converges to zero in a simulation carried out starting from perturbed initial conditions using EPD-PBC with $k_{pd} = 8.4$. As highlighted by the box on the right, the value of the storage function at every impact is less than (or equal to) the value at the previous impact.

sake of comparison, the same initial conditions have been used to test performances of the min-norm control (MNC) employed in [18]. Results of simulations with the EPD-PBC and the MNC have been collected in TABLE I, where *PG* indicates the passive gait while *NG* indicates a new gait characterized by $S_N = 0.5351\ m$, $T_N = 0.7282\ s$, and $H_N = 153.12\ J$. Control gains have been firstly tuned to face uniform disturbances. Then, they have been tested in all ten simulations. Those reported in the table are the best ones for each methodology ($k_{mn} = c/\varepsilon$ with $c = 1$ and $\varepsilon = 0.5$, see [18] for further details). By inspecting TABLE I, it is

x_{0P}	EPD-PBC	MNC
	$k_{pd} = 1$	$k_{mn} = 2$
1	-	-
2	PG	NG
3	PG	-
4	-	-
5	-	-
6	PG	-
7	-	NG
8	-	NG
9	-	-
10	PG	NG

TABLE I

CASE STUDY I. COMPARISON BETWEEN EPD-PBC AND MNC

clear that both methodologies increase the CBR's robustness to initial conditions. EPD-PBC is more suitable to increase the basin of attraction of the passive limit cycle, compared to MNC. The passive gait has been recovered in 4 out of 10 total trials, with $k_{pd} = 1$. On the other hand, MNC never succeeds to recover the passive limit cycle, as evident by the new gait created. MNC cannot enlarge the basin of attraction of the passive limit cycle for perturbations equal or greater than those considered in this paper. Another crucial aspect is that EPD-PBC avoids robot falling as many times as done by MNC. In conclusion, EPD-PBC exhibits the same performances of MNC in increasing the overall robustness, but it is more effective in recovering the passive gait, as a consequence of the almost global stability results obtained via invariant sets theory.

B. Case Study II

Now, EPD-PBC has been applied after energy shaping. The energy of the system has been shaped through the IDA-PBC procedure proposed in [29]. Such a methodology was already deployed in [16] to tackle the CBR gait generation problem. Energy-shaping is motivated by the possibility to generate new gaits. As remarked in [3], the gait exhibited by a CBR emerges from its particular inertial and geometrical properties. If both inertia and geometry are fixed, as well as the slope of the incline, the energy flow between the walking surface and the robot is fixed too, driving biped dynamics towards its passive limit cycle with energy H_P. As shown in [4], control approaches similar to EPD-PBC and MNC fail in stabilizing target energies values which significantly differs from H_P (*i.e.*, $H^* >> H_P$ or $H^* << H_P$). In some cases, the resulting gait is exactly the passive one while, in others, new gaits arise, whose energies are different. Then, to stabilize a desired H^*, it is necessary to change how the robot and the ground interact, modifying both the inertial and the geometrical properties of the biped. Therefore, its kinetic and potential energies must be shaped.

A novel gait has been generated via an inner IDA-PBC control loop. Since it is not required to add dissipation in this task, the damping-injection step has been skipped. Hence, IDA-PBC has been reduced to the energy shaping phase only. The obtained gait has $S_{ida} = 0.5329\ m$ and $T_{ida} = 0.7717\ s$ as parameters, while its energy is $H_{ida} = 227.8194\ J$. Notice how this gait is significantly slower than the passive one. The same procedure adopted in [16] has been followed, appropriately adapted to take into account the actuation at the hip instead of at the ankle. Simulation has been performed starting from $\begin{bmatrix}0.1959 & -0.2902 & -0.9576 & -0.2700\end{bmatrix}^T$, which corresponds to a uniform 10% perturbation on the passive initial conditions $x_{0ida} = \begin{bmatrix}0.2177 & -0.3224 & -1.0640 & -0.3000\end{bmatrix}^T$, without introducing the proposed EPD-PBC. The CBR falls after few simulation seconds, showing that this novel limit cycle has a very narrow basin of attraction.

Then, an outer EPD-PBC loop, with $k_{pd} = 0.7$ and $H^* = 227.8194\ J$ has been implemented. As shown in Fig. 5, the limit cycle (blue line) converges to the target one (green line) which partially surrounds the passive one (red line) placed here as a reference. Thanks to the EPD-PBC, the CBR keeps walking, demonstrating its usefulness to increase the robustness of newly generated gaits.

VI. CONCLUSION AND FUTURE WORK

In this paper, a control design using EPD-PBC with HZD for planar passive bipeds was proposed. It was shown that the passive gait, and the gaits generated through energy shaping, can be robustified by using the proposed design. Numerical simulations validated the approach.

A limitation of the proposed solution is that it is suited only for passive-dynamic walking (*i.e.*, the biped already exhibits a passive periodic gait). Future work will focus on

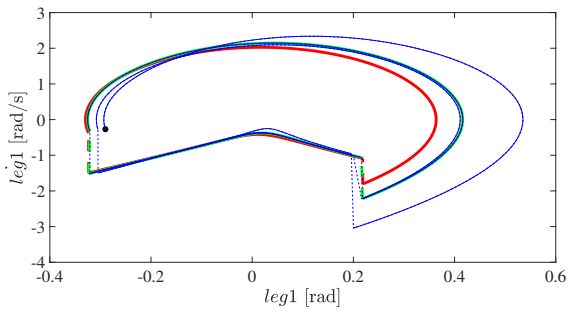

Fig. 5. Case Study II. Limit cycles comparison for leg1. Red arcs represent the passive limit cycle without energy shaping. Green arcs represent the gait generated through IDA-PBC starting from nominal initial conditions. Blue arcs represent the same gait starting from perturbed initial conditions. Black dot represents perturbed initial conditions. Blue arcs converge to green ones using EPD-PBC with $k_{pd} = 1$.

applying the presented methodology to a planar biped robot with more degrees of freedom and extend the methodology to bipeds that are not constrained to move in the sagittal plane only.

REFERENCES

[1] T. McGeer, "Passive dynamic walking," *The International Journal of Robotics Research*, vol. 9, no. 2, pp. 62–82, 1990.

[2] T. McGeer, "Passive walking with knees," in *Proceedings., IEEE International Conference on Robotics and Automation*, vol. 3, 1990, pp. 1640–1645.

[3] A. Goswami, B. Thuilot, and B. Espiau, "Compass-like biped robot Part I: Stability and bifurcations of passive gaits," *Institut National de Recherche en Informatiqu et en Automatique (INRIA),Techical Report 2996*, 1996.

[4] A. Goswami, B. Espiau, and A. Keramane, "Limit cycles in a passive compass gait biped and passivity-mimicking control laws," *Autonomous Robots*, no. 4, pp. 273–286, 1997.

[5] A.-D. Kuo, "Energetics of actively powered locomotion using the simplest walking model ," *Journal of Biomechanical Engineering*, vol. 124, no. 1, pp. 113–120, 09 2001.

[6] A. Kuo, "The six determinants of gait and the inverted pendulum analogy: A dynamic walking perspective," *Human Movement Science*, vol. 26, no. 4, pp. 617–656, 2007.

[7] V. De-León-Gómez, V. Santibanéz, and J. Sandoval, "Interconnection and damping assignment passivity-based control for a compass-like biped robot," *International Journal of Advanced Robotic Systems*, vol. 14, no. 4, 2017.

[8] R. Ortega, A. Donaire, and J. G. Romero, *Passivity-based control of mechanical systems*, ser. Feedback Stabilization of Controlled Dynamical Systems–In Honor of Laurent Praly, Lecture Notes in Control and Information Sciences. Berlin/Heidelberg: Springer, 2017, pp. 167–199.

[9] M. W. Spong and F. Bullo, "Controlled symmetries and passive walking," in *Proceeding IFAC Triennal World Congress*, Barcelona, Spain, 2002.

[10] M. W. Spong and G. Bhatia, "Further results on control of the compass gait biped," in *2003 IEEE/RSJ International Conference on Intelligent Robots and Systems*, Las Vegas, NV, USA, 2003, pp. 1933–1938.

[11] M. W. Spong, J. Holm, and D. Lee, "Passivity-based control of bipedal locomotion," in *IEEE Robotics & Automation Magazine*, vol. 12, no. 2, 2007, pp. 30–40.

[12] J. Holm and M. W. Spong, "Kinetic energy shaping for gait regulation of underactuated bipeds," in *IEEE International conference on control applications*, San Antonio, Texas, USA, 2008, pp. 1232–1238.

[13] V. Duindam, "Port-Based Modelling and Control for Efficient Bipedal Walking Robots," Ph.D. dissertation, Ph.D. Dissertation, University of Twente, 2006.

[14] R. Ortega, A. Van Der Schaft, I. Mareels, and B. Maschke, "Putting energy back into control," *IEEE Control Systems Magazine*, pp. 18–33, 2001.

[15] R. Ortega, A. Van Der Schaft, B. Maschke, and G. Escobar, "Interconnection and damping assignment passivity-based control of port-controlled Hamiltonian systems," *Automatica*, vol. 38, no. 4, pp. 585–596, 2002.

[16] P. Arpenti, F. Ruggiero, and V. Lippiello, "Interconnection and damping assignment passivity-based control for gait generation in underactuated compass-like robots," in *2020 IEEE International Conference on Robotics and Automation*, Paris, France, 2020, pp. 9802–9808.

[17] J. W. Grizzle, C. Chevallereau, R. W. Sinnet, and A. D. Ames, "Models, feedback control, and open problems of 3d bipedal robot walking," *Automatica*, vol. 50, no. 8, pp. 1955–1988, 2014.

[18] R. W. Sinnet and A. D. Ames, "Energy shaping of hybrid systems via control lyapunov functions," in *2015 American Control Conference*, Chicago, IL, 2015, pp. 5992–5997.

[19] A. D. Ames, K. Galloway, K. Sreenath, and J. W. Grizzle, "Rapidly Exponentially Stabilizing Control Lyapunov Functions and Hybrid Zero Dynamics," *IEEE Transactions on Automatic Control*, vol. 59, no. 4, pp. 876–891, 2014.

[20] E. R. Westervelt, J. W. Grizzle, and D. E. Koditschek, "Hybrid zero dynamics of planar biped walkers," *IEEE Transactions on Automatic Control*, vol. 48, no. 1, pp. 42–56, 2003.

[21] E. R. Westervelt, J. W. Grizzle, C. Chevallereau, J. H. Choi, and B. Morris, *Feedback control of dynamic bipedal robot locomotion*. London, UK: Taylor & Francis/CRC Press, 2007.

[22] B. Morris and J. W. Grizzle, "Hybrid invariant manifolds in systems with impulse effects with application to periodic locomotion in bipedal robots," *IEEE Transactions on Automatic Control*, vol. 54, no. 8, pp. 1751–1764, 2009.

[23] H. Sadeghian, C. Ott, G. Garofalo, and G. Cheng, "Passivity-based control of underactuated biped robots within hybrid zero dynamics approach," in *2017 IEEE International Conference on Robotics and Automation (ICRA)*, Singapore, 2017, pp. 4096–4101.

[24] K. J. Astrom, J. Aracil, and F. Gordillo, "A family of smooth controllers for swinging up a pendulum," *Automatica*, vol. 44, no. 7, pp. 1841–1848, July 2008.

[25] B. Yi, R. Ortega, D. Wu, and W. Zhang, "Orbital stabilization of nonlinear systems via Mexican sombrero energy shaping and pumping-and-damping injection," *Automatica*, vol. 112, 2020.

[26] M. Nacusse, P. Arpenti, F. Ruggiero, and V. Lippiello, "Gait generation for underactuated compass-like robots using dissipative forces in the controller," *IFAC-PapersOnLine*, vol. 53, no. 2, pp. 9023–9030, 2020.

[27] H. K. Khalil, *Nonlinear systems; 3rd ed.* Upper Saddle River, NJ: Prentice-Hall, 2002.

[28] Ö. Karabacak, R. Wisniewski, and J. Leth, "On the almost global stability of invariant sets," in *2018 European Control Conference*, 2018, pp. 1648–1653.

[29] D. Serra, F. Ruggiero, A. Donaire, L. Buonocore, V. Lippiello, and B. Siciliano, "Control of nonprehensile planar rolling manipulation: A passivity based approach," *IEEE Transactions on Robotics*, vol. 35, no. 2, pp. 317–329, 2019.